MOLECULAR PHYSICS, 1997, VOL. 92, NO. 3, 429–439

An *ab initio* study of anharmonicity and matrix effects on the hydrogen-bonded BrH:NH_3 complex

By JANET E. DEL BENE
Department of Chemistry, Youngstown State University, Youngstown, OH 44555, USA

MEREDITH J. T. JORDAN, PETER M. W. GILL and A. DAVID BUCKINGHAM
Department of Chemistry, University of Cambridge, Cambridge CB2 1EW, UK

(*Received 25 March 1997; accepted 26 May 1997*)

Ab initio calculations have been carried out to investigate the structure and infrared spectrum of BrH:NH_3, and to resolve the discrepancies found between its computed harmonic and experimental spectrum. MP2/6-31+G(d, p) and MP2/aug′-cc-pVDZ potential surfaces have been constructed, and a model two-dimensional nuclear vibrational problem has been solved to obtain the fundamental dimer stretching and proton stretching frequencies. These vibrational modes are strongly coupled anharmonic modes. The anharmonic proton stretching frequencies are lower than the harmonic by 1100 and 900 cm^{-1} respectively at the two levels of theory and are in better agreement with the experimental frequency. The argon matrix alters the potential energy surface by preferentially stabilizing the more polar proton-shared structure over the structure with a traditional hydrogen bond.

1. Introduction

Ab initio calculations using second-order Møller–Plesset (MP2) perturbation theory with the 6-31+G(d, p) basis set have been successful in describing the structures and vibrational spectra of hydrogen-bonded complexes with traditional X-H···Y hydrogen bonds. At this level, intermolecular distances agree satisfactorily with distances measured in the gas phase, and observed red shifts of the X–H stretching band upon formation of the X-H···Y hydrogen bond are usually satisfactorily reproduced [1]. However, there are some complexes for which significant discrepancies have been found between computed spectra and experimental spectra obtained in inert-gas matrices. One such complex is that formed between HBr and NH_3. Moreover, experimental data present apparently conflicting descriptions of the type of hydrogen bond in this complex. Howard and Legon [2] obtained the structure of BrH:NH_3 using microwave spectroscopy and described this complex as one with a traditional hydrogen bond. In contrast, the infrared spectrum of BrH:NH_3 obtained in an argon matrix suggests the presence of a proton-shared hydrogen bond.

We have undertaken a detailed study of the BrH:NH_3 system in an effort to resolve these discrepancies and to understand hydrogen bonding in this complex. Our aim is to answer the following questions.

(1) What is the nature of the BrH:NH_3 potential energy surface?
(2) What are the fundamental anharmonic frequencies for the dimer and proton stretching modes in BrH:NH_3, and how do these frequencies compare with the corresponding harmonic frequencies?
(3) How do inert gas atoms influence the structure and vibrational spectrum of BrH:NH_3?

2. Methods

The structures of the complexes BrH:NH_3 and BrH:NH_3:3Ar have been fully optimized with correlation using MP2 perturbation theory [3–6] with the 6-31+G(d, p) basis set [7–10]. Two equilibrium BrH:NH_3 structures and the transition-state structure connecting these were found, all structures having C_{3v} symmetry. The equilibrium BrH:NH_3:3Ar complex also has C_{3v} symmetry, with the argon atoms staggered with respect to the ammonia hydrogen atoms, as illustrated in figure 1. Harmonic vibrational frequencies were computed to identify equilibrium and transition structures and to predict the vibrational spectrum. For the BrH:NH_3 complex, a potential curve was generated for proton motion along the normal coordinate corresponding to the Br–H stretch. This curve was also computed in the presence of

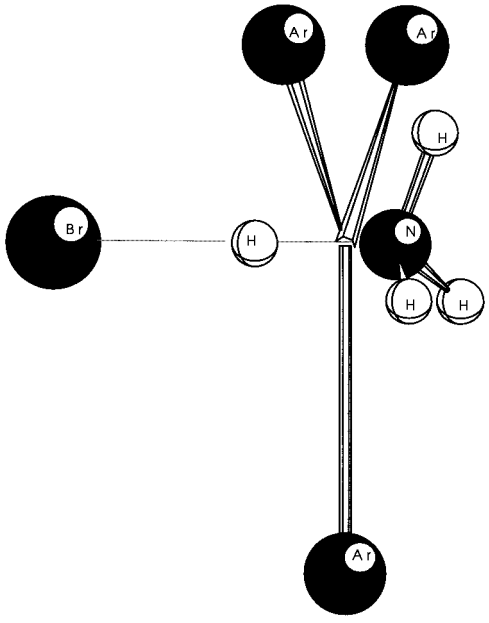

Figure 1. The equilibrium structure of BrH:NH_3:3Ar.

electric fields, with the field strength varying from 0·0025 to 0·0125 au, in steps of 0·0025 au. The weaker fields are consistent with what might be induced within an argon matrix by a polar species. The curve for proton motion along the normal coordinate in the BrH:NH_3:3Ar complex was also computed.

The potential energy surface in the hydrogen-bonding region of BrH:NH_3 was generated at the MP2/6-31+G(d, p) level of theory from about 550 grid points. Since the hydrogen bond is linear in both the 'short' and the 'long' Br–H bond equilibrium structures, the surface in the hydrogen-bonding region was described in terms of two hydrogen-bonding coordinates: R_1, the N–H distance, and R_2, the Br–H distance. For these calculations, the geometry of NH_3 was frozen at an N–H distance of 1·015 Å and an H–N–H angle of 110·6°. These are the average values of the two equilibrium structures. Freezing the NH_3 geometry results in destabilization of the equilibrium complexes by only 0·04 kcal mol^{-1}. The potential surface in the hydrogen-bonding region of BrH:NH_3:3Ar for Br–N distances between 2·92 and 3·00 Å was also obtained. Again, the geometry of NH_3 was fixed at its geometry in the optimized complex, and the distance from bromine to the plane of the argon atoms was frozen at the equilibrium distance. These constraints have negligible energy effects.

It is known that the calculation of reliable hydrogen-bond energies requires a basis set larger than 6-31+G(d, p). Improved energetics can be obtained from single-point calculations at MP2/6-31+G(d, p) geometries using the augmented correlation-consistent polarized split-valence basis sets of Dunning and co-workers [11–13]. These basis sets are denoted as aug-cc-pVXZ, where X = D for double, T for triple, Q for quadruple and 5 for quintuple split, and aug′-cc-pVXZ, which is aug-cc-pVXZ without diffuse functions on hydrogen atoms. Although MP2/aug′-cc-pVTZ is the recommended level of theory for computing consistently reliable energetics in both neutral and charged hydrogen-bonded complexes, MP2/aug′-cc-pVDZ hydrogen-bond energies for neutral complexes have been found to be reasonable, and usually similar to MP2/aug′-cc-pVTZ energies [1]. Single-point MP2/aug′-cc-pVDZ and MP2/aug′-cc-pVTZ calculations have been carried out on both equilibrium BrH:NH_3 structures found on the MP2/6-31+G(d, p) surface. The BrH:NH_3 complex was also optimized at the MP2/aug′-cc-pVDZ level, and the potential surface was computed at this level. All MP2 calculations reported in this work were done freezing s and p electrons below the valence shells in the Hartree–Fock (HF) molecular orbitals.

Two-dimensional anharmonic vibrational frequencies were calculated using the method outlined by Wei and Carrington [14]. For a collinear A–B–C system the two-dimensional model vibrational Hamiltonian is given by (for example [15])

$$H = -\frac{\hbar^2}{2\mu_1}\frac{\partial^2}{\partial R_1^2} - \frac{\hbar^2}{2\mu_2}\frac{\partial^2}{\partial R_2^2} + \frac{\hbar^2}{m_B}\frac{\partial^2}{\partial R_1\,\partial R_2} + V(R_1, R_2), \quad (1)$$

where R_1 is the AB bond length, R_2 is the BC bond length, $1/\mu_1 = 1/m_A + 1/m_B$, $1/\mu_2 = 1/m_B + 1/m_C$, and m_X is the mass of the moiety X. In this case, A is identified as NH_3, B as the H atom and C as the Br atom, with R_1 representing the N–H distance and R_2 the Br–H distance. Only the coordinates R_1 and R_2 were varied, and no account was taken of bending motions.

A two-dimensional study has been performed previously on the BrH:NH_3 system at the HF/double zeta plus polarization (DZP) level of theory [16]. Although this study indicated the importance of anharmonic effects, the HF/DZP level of theory and the nature of the polynomial expansion used to fit the two-dimensional potential energy surface were not adequate to obtain reliable vibrational frequencies.

The two-dimensional basis functions used in the present study consisted of products of one-dimensional functions optimized by solving appropriate one-dimensional Schrödinger equations for R_1 and R_2. Tridiagonal Morse functions [14, 17] were used as a primitive basis with the matrix elements of the kinetic energy operator terms calculated using analytical formulae [14, 18]. The

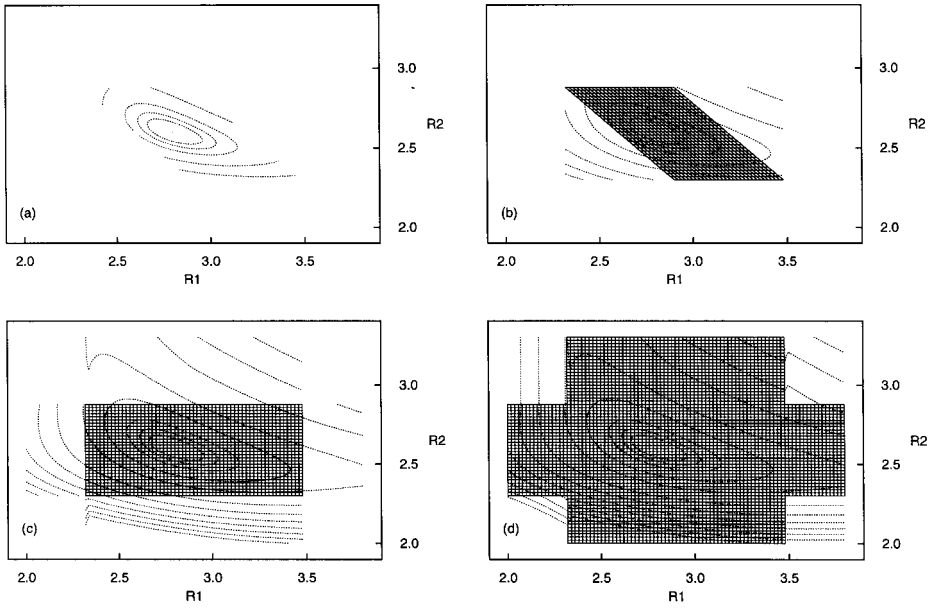

Figure 2. Diagrammatic representations of the scheme used to construct a global potential energy surface from discrete *ab initio* energies in the distances R_1 and R_2: (*a*) the initial *ab initio* energies; (*b*) the augmented grid in (R_1, R_2); (*c*) polynomial extrapolations off the sides of the augmented grid; (*d*) linear expolations off the corners of the augmented grid.

final basis sets used in the variational calculations of the vibrational eigenvalues of BrH:NH$_3$ had dimension 3600 with ratios of 120:60 primitive:contracted basis functions in both R_1 and R_2 coordinates and yielded eigenvalues converged to better than 0·5 cm^{-1}.

Global potential energy surfaces $V(R_1, R_2)$ for use in the two-dimensional calculations were constructed from initial grids of *ab initio* data using both interpolating and extrapolating functions. The procedure used is described below and illustrated diagrammatically in figure 2.

For both basis sets considered, the initial *ab initio* points were calculated at fixed $R_1 + R_2$ distances, yielding a parallelogram of data on the (R_1, R_2) plane (figure 2(*a*)). The initial $(R_1 + R_2, R_2)$ grid was first extrapolated in the R_1 coordinate to yield a rectangular 'augmented' grid in (R_1, R_2) (figure 2(*b*)). For fixed values of R_2, quadratic extrapolation was used for R_1 distances shorter than those in the $(R_1 + R_2, R_2)$ grid and linear extrapolation for longer R_1 distances. The augmented grid, defined by $R_1^{\min} < R_1 < R_1^{\max}$ and $R_2^{\min} < R_2 < R_2^{\max}$, was then used to construct the potential surface. A two-dimensional spline interpolation was used to calculate energies within the augmented grid, quadratic extrapolation was used to calculate energies off the short sides of the grid (i.e. for $R_1 < R_1^{\min}$ or $R_2 < R_2^{\min}$, and linear extrapolation to calculate energies off the long sides of the grid. The resulting potential energy surface is illustrated in figure 2(*c*).

The potential off the corners of the augmented grid was determined as follows. For coordinates (R_1, R_2), where one of the coordinates was short and the other long, a constant extrapolation was used along the short bond length. For example, if $R_1 < R_1^{\min}$ and $R_2 > R_2^{\max}$, then $V(R_1, R_2) = V(R_1, R_2^{\max})$. A linear interpolation with a slope of - 1 was used from the extrapolated grid sides in the 'near' and 'far' corners. For example, if $R_1 < R_1^{\min}$ and $R_2 < R_2^{\min}$, then

$$V(R_1, R_2) = v_1 + (v_2 - v_1)\frac{R_1^{\min} - R_1}{R_1^{\min} - R_1 + R_2^{\min} - R_2}, \quad (2)$$

where $v_1 = V(R_1 + R_2 - R_2^{\min}, R_2^{\min})$ and $v_2 = V(R_1^{\min}, R_1 + R_2 - R_1^{\min})$.

The final calculated potential is illustrated in figure 2(*d*). Figure 2(*d*) indicates that small non-physical variations may occur in the potential arising from either the spline interpolation at the grid boundaries or the extrapolation procedure. The original data set was sufficiently large to ensure that these variations occurred at relatively high energies and do not affect the calculated vibrational frequencies.

The E01DAF and E02DFF NAG routines [19] were used to perform the two-dimensional spline interpolations. Polynomial extrapolating functions were fitted to the appropriate number of points interpolated within the data grid (with either R_1 or R_2 fixed) at increments δR from the grid boundary. For example, if $R_1 < R_1^{\min}$ and $R_2^{\min} < R_2 < R_2^{\max}$, then $V(R_1, R_2) = f(R_1)$, where $f(R_1)$ is a quadratic fit to the potential at the three points $(R_1^{\min}, R_2)$, $(R_1^{\min} - \delta R, R_2)$ and $(R_1^{\min} - 2\delta R, R_2)$. A value of $\delta R = 0{\cdot}01$ bohr was used in the calculations described below.

The sensitivity of the calculated vibrational eigenvalues to the order of the polynomial extrapolating functions and to the value of δR was investigated. Because of the curvature of the potential surface, only zeroth order and linear extrapolations were considered

Table 1. Selected MP2/6-31+ G(d, p) structural, energy and harmonic spectral data for BrH:NH_3 complexes: (T), 'traditional' hydrogen-bonded structures; (PS), 'proton-shared' hydrogen-bonded structures.

Complex	R(Br–N)/Å	r(Br–H)/Å	d(Br–X)[a]/Å	d(X–Ar)[a]/Å	ΔE/(kcal mol^{-1})	υ/cm^{-1}	I/(km mol^{-1})
BrH:NH_3 (T)	3·247	1·462			- 10·0	2006	1948
BrH:NH_3 (PS)	2·971	1·718			- 9·1	387	2329
						414	2927
BrH:NH_3:3Ar	2·966	1·741	2·532	3·544	- 12·4	716	4617
Experiment	3·255[b]					729[c]	

[a] Br–X is the distance from the bromine atom to the plane of the argon atoms; X–Ar is the perpendicular distance from an argon atom to the Br–N line.
[b] The gas-phase Br–N distance from [2].
[c] The proton stretching frequency in the experimental spectrum obtained at 10 K in an argon matrix.

at long bond lengths. In this case, variations of 0·5, 12 and 15 cm^{-1} were observed in the zero-point energy, the first dimer stretching vibrational eigenvalue and the first proton stretching eigenvalue respectively. Varying the order of the extrapolating polynomial between 2 and 6 at short bond lengths varied the calculated vibrational eigenvalues by less than 2·5 cm^{-1}. Changing the parameter δR by an order of magnitude resulted in changes to the vibrational eigenvalues of less than 1 cm^{-1}. The sensitivity analysis demonstrates the robustness of the potential energy surface and indicates that the initial *ab initio* data points chosen provide a good description of the regions of the potential surface important for hydrogen bonding.

It was not possible to construct a two-dimensional potential energy surface for the BrH:NH_3:3Ar system. Instead, a one-dimensional anharmonic wavefunction was considered along the harmonic normal mode displacement vector for the proton stretching vibration. The one-dimensional Hamiltonian was simply

$$H = -\frac{\hbar^2}{2m_H}\frac{\partial^2}{\partial R^2} + V(R), \qquad (3)$$

where the coordinate R parameterizes the potential slice along the normal coordinate and the proton is considered to move under the influence of the potential $V(R)$. The potential is defined by a one-dimensional spline interpolation through a discrete set of *ab initio* potential energies calculated along the normal mode displacement vector and the polynomial extrapolation of the potential outside the initial data set. As previously, tridiagonal Morse functions were used to expand the vibrational wavefunctions, and anharmonic energy levels were calculated using 200 basis functions. The uncertainties in the calculated eigenvalues due to the potential extrapolation procedure were estimated to be 2 cm^{-1} for the zero-point energy and 20 cm^{-1} for the first excited state.

The optimization and harmonic frequency calculations were carried out using the Gaussian 94 suite of computer programs [20]. The potential curves and surfaces were generated using Gaussian 94 and Q-CHEM [21]. These calculations were carried out on the SGI-PC and Cray Y-MP8E/128 computers at the Ohio Supercomputer Center, and the Theoretical Chemistry computing facilities at the University of Cambridge.

3. Results and discussion

Table 1 presents the computed MP2/6-31+ G(d, p) Br–N and Br–H distances, electronic binding energies, and harmonic frequencies and intensities for the proton stretching mode for the three complexes. The more stable BrH:NH_3 complex (BrH:NH_3 (T), where (T) designates a traditional hydrogen bond) has a binding energy of 10·0 kcal mol^{-1}. In this complex, the computed rotational constant B_e is 3237 MHz using the standard isotopic masses for ^{1}H (1·0078 amu), ^{14}N (14·0031 amu) and ^{79}Br (78·9183 amu). The Br–N distance R_e (the distance at the minimum on the potential energy surface) is 3·247 Å, and the Br–H distance is 1·462 Å. This structure is similar to that computed by Latajka *et al.* [22]. Howard and Legon [2] have reported the microwave spectrum of the BrH:NH_3 complex. They obtained a rotational constant B_0 of 3227 MHz for the same isotopes and deduced a Br–N distance R_0 (the Br–N distance in the ground vibrational state) of 3·255 Å. These values are consistent with the computed values. On the basis of their observations, Howard and Legon [2] described this complex as one with a 'traditional' hydrogen bond.

The computed Br–H harmonic stretching frequency (expressed in wavenumbers) in BrH:NH_3 (T) occurs at 2006 cm^{-1}, red shifted from monomeric HBr by 726 cm^{-1}. The magnitude of this shift is consistent with shifts in complexes with traditional hydrogen bonds [23]. However, the computed spectrum of BrH:NH_3 is significantly different from the experimental spectrum obtained in an argon matrix at 10 K, which shows a strong band at 729 cm^{-1}. The computed

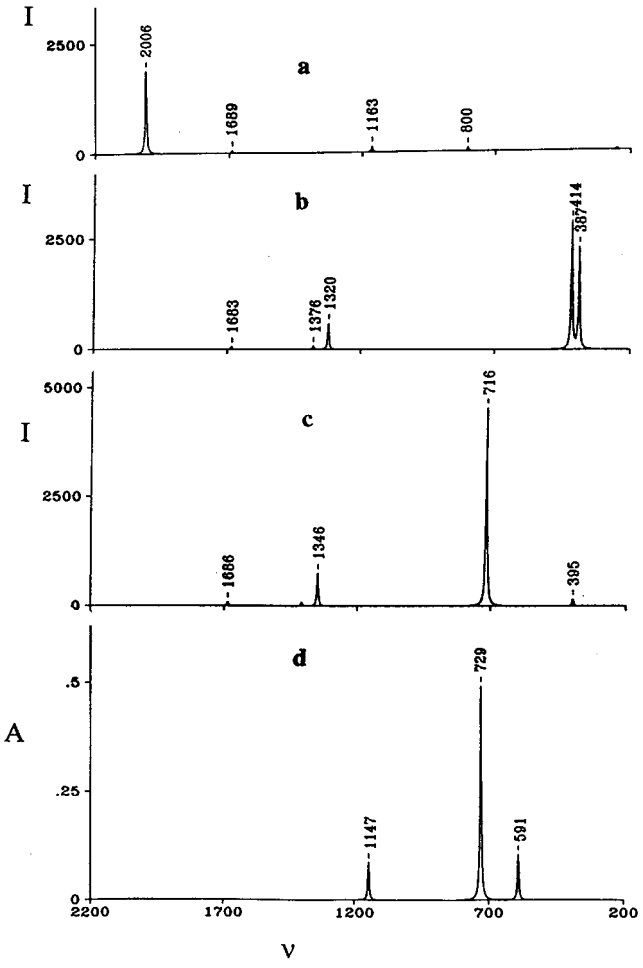

Figure 3. Vibrational spectra with frequencies υ in cm^{-1} and intensities I in km mol^{-1}. (*a*) The computed spectrum of BrH:NH$_3$ (T). All computed spectra in this figure were calculated at MP2/6-31+G(d, p) within the harmonic approximation. (*b*) The computed spectrum of BrH:NH$_3$ (PS). (*c*) The computed spectrum of BrH:NH$_3$:3Ar. (*d*) The experimental BrH:NH$_3$ spectrum at 10 K in an argon matrix after subtraction of the monomer spectra. The spectrum shown is an integrated intensity sum spectrum with A representing per cent absorbance.

BrH:NH$_3$ (T) vibrational spectrum and the experimental spectrum are shown in figure 3.

A second equilibrium structure (BrH:NH$_3$ (PS), where PS designates a 'proton-shared' hydrogen bond) has been found on the intermolecular surface. This structure is 0·9 kcal mol^{-1} less stable than BrH:NH$_3$ (T). It has a significantly shorter Br–N distance R_e of 2·971 Å, and a longer Br–H distance of 1·718 Å. The structure of BrH:NH$_3$(PS) is typical of complexes with proton-shared Br…H…N hydrogen bonds [23] As expected, the spectrum of this complex is dramatically different from that of BrH:NH$_3$(T), exhibiting two strong bands of approximately equal intensity at 414 and 387 cm^{-1}. As evident from figure 3, this spectrum also does not agree with the experimental argon matrix spectrum, which is dominated by one intense low-frequency band.

Although BrH:NH$_3$ (PS) is a local minimum on the surface, the barrier to proton transfer to form BrH:NH$_3$ (T) is less than 0·01 kcal mol^{-1}. This barrier is below the zero-point vibrational energy for the proton stretching mode. Therefore BrH:NH$_3$ (PS) is a Born–Oppenheimer minimum which is not stable. However, since the energy of BrH:NH$_3$ (PS) is only 0·9 kcal mol^{-1} higher than that of BrH:NH$_3$ (T), the potential curve for the proton stretching motion in BrH:NH$_3$ (T) is noticeably anharmonic, as evident from the zero-field curve in figure 4. Large-amplitude motion of the hydrogen-bonded proton can be expected.

Before the BrH:NH$_3$ surface is examined in detail, the BrH:NH$_3$:3Ar complex will be considered. Table 1 reports structural, energy and vibrational data for this complex. Relative to HBr and NH$_3$:3Ar, BrH:NH$_3$:3Ar has a binding energy of 12·4 kcal mol. It has a decreased intermolecular Br–N distance R_e of 2·966 Å and an increased Br–H distance to 1·741 Å relative to BrH:NH$_3$ (T) and is structurally similar to BrH:NH$_3$ (PS). As evident from figure 3, the computed harmonic spectrum of this complex is in agreement with the experimental spectrum, with one intense low-frequency band for the proton stretching mode at 716 cm^{-1}. Thus the presence of the argon atoms has dramatic structural and spectral effects, changing the

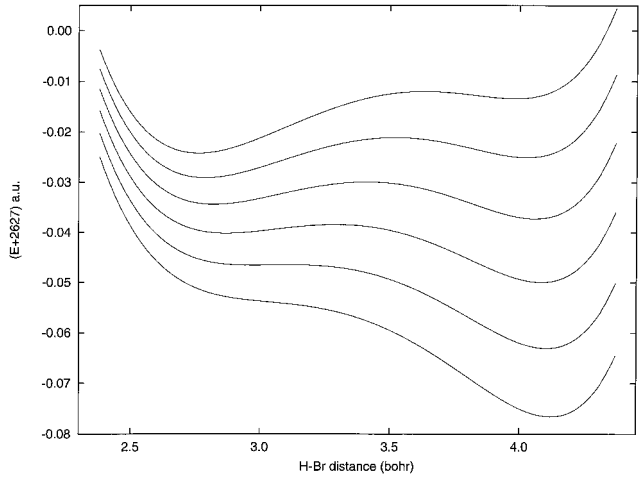

Figure 4. MP2/6-31+G(d, p) potential energy curves along the normal coordinate for the proton stretching mode in BrH:NH$_3$ (T). Successive curves correspond to increasing field strength in the Br–H direction, beginning with zero field at the top and incrementing the field in steps of 0·0025 au.

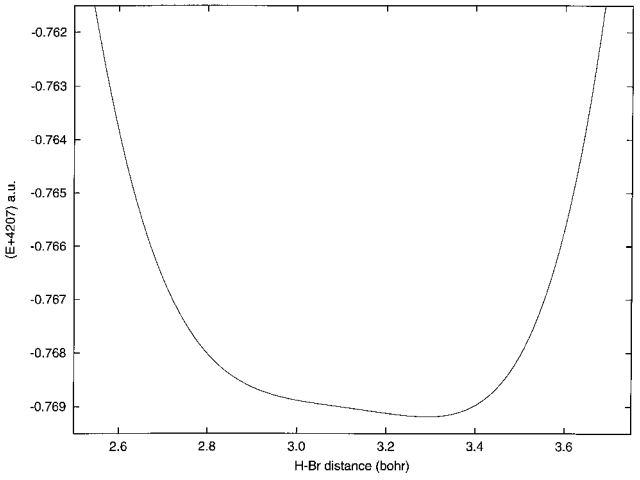

Figure 5. MP2/6-31+G(d, p) potential energy curve along the normal coordinate for the proton stretching mode in BrH:NH_3:3Ar.

hydrogen bond type from traditional to proton shared, and producing a vibrational spectrum in agreement with experiment. The potential curve for the proton stretching mode along the normal coordinate in BrH:NH_3:3Ar is shown in figure 5. This curve has a single minimum and is flat, so that the proton can undergo large displacements along this coordinate with small energy consequences.

In order to compute the anharmonic frequencies for the dimer stretching and proton stretching modes, a global BrH:NH_3 potential energy surface was first determined from approximately 550 single-point calculations at the MP2/6-31+G(d, p) level of theory. The original data points are illustrated in figure 6. The initial augmented grid (figure 2(*b*)) was further supplemented by points calculated along the HBr + NH_3 asymptote and in the proton-shared region. These points were added to ensure that the initial data were sufficiently extensive to prevent errors in the calculated eigenvalues due to the extrapolation procedure. The final potential surface is illustrated in figure 7, where the traditional and proton-shared minima are indicated by asterisks. Evident on this surface are Morse-type curves for the dissociation of the complex to HBr and NH_3, and a valley connecting BrH:NH_3 (T) and BrH:NH_3 (PS). The dimer and proton stretching modes are coupled together through the two-dimensional Hamiltonian (equation (1)), and the resulting ground-state wavefunction exhibits large-amplitude motion in the valley, as illustrated in figure 8.

The anharmonic zero-point vibrational energy computed from this surface is 2·2 kcal mol^{-1}, allowing the ground-state BrH:NH_3 vibrational wavefunction to sample both the BrH:NH_3 (T) and the BrH:NH_3 (PS)

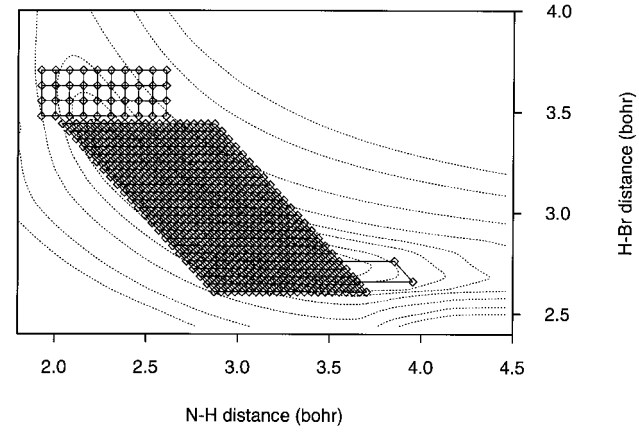

Figure 6. The potential energy surface for BrH:NH_3 at the MP2/6-31+G(d, p) level of theory. The initial *ab initio* points used to define the surface are indicated.

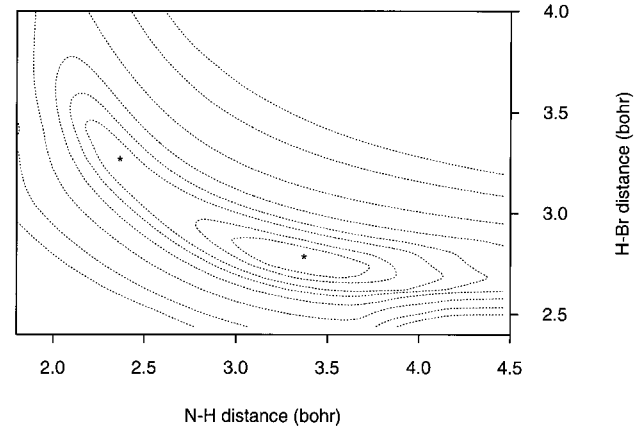

Figure 7. The MP2/6-31+G(d, p) potential energy surface for BrH:NH_3 with the two calculated minima indicated as asterisks. Potential energy contours are at energies 0·0005, 0·001, 0·002, 0·003, 0·005, 0·01, 0·02 and 0·03 au above the global minimal energy.

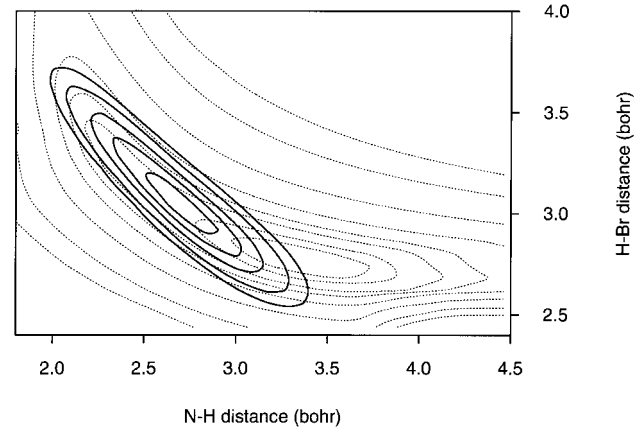

Figure 8. The square of the ground-state vibrational wavefunction superimposed on the MP2/6-31+G(d, p) potential surface, with contours as in figure 7. The zero-point energy is 786 cm^{-1}.

Table 2. Two-dimensional anharmonic data for BrH:NH$_3$ complexes (results obtained using 3600 basis functions), where $\langle x \rangle$ denotes the expectation value of x.

	Total energy/hartrees	$\upsilon(E - E_0)$/cm^{-1}	$\langle R_1 \rangle$/Å	$\langle R_2 \rangle$/Å	$\langle R_0 \rangle$/Å
MP2/6-31+G(d, p)					
Ground state	- 2627·020 58	0	1·428	1·624	3·053
Dimer stretch	- 2627·019 59	218	1·555	1·571	3·126
Proton stretch	- 2627·016 54	888	1·368	1·714	3·082
MP2/aug′-cc-pVDZ					
Ground state	- 2629·535 15	0	1·532	1·572	3·104
Dimer stretch	- 2629·534 35	176	1·611	1·552	3·162
Proton stretch	- 2629·530 11	1106	1·382	1·706	3·088

wells. The wavefunction is centred between these two minima in a relatively flat region of the potential energy surface. The expectation value of the Br–N distance R_0 is 3·05 Å, considerably shorter than the 3·255 Å distance deduced by Howard and Legon [2]. The anharmonic fundamental vibrational excitations for the dimer stretching mode and the proton stretching mode are 218 and 888 cm^{-1}. The excited-state wavefunctions are shown superimposed on the potential energy surface in figures 9 and 10. In the harmonic approximation these modes for BrH:NH$_3$ (T) were found at 135 and 2006 cm^{-1} respectively. Thus the anharmonic stretching frequency for the Br–H stretch is lower than the harmonic value by more than 1000 cm^{-1}. Although the computed anharmonic frequency is still higher than the experimental argon matrix frequency by about 150 cm^{-1}, the agreement between theory and experiment is now reasonable. The anharmonic data are summarized in table 2.

The expectation value R_0 for the BrH:NH$_3$ complex obtained from the MP2/6-31+G(d, p) surface is not consistent with the Br–N distance found by Howard and Legon [2]. This may be due in part to the tendency of the 6-31+G(d, p) basis set to overestimate binding energies, particularly of the more polar BrH:NH$_3$ (PS) structure. This is supported by the single-point MP2/aug′-cc-pVDZ and MP2/aug′-cc-pVTZ binding energies which are reported in table 3. The binding energies of both structures are reduced with these larger basis sets, but the binding energy of the proton-shared structure is more sensitive, so that improving the basis set reduces its

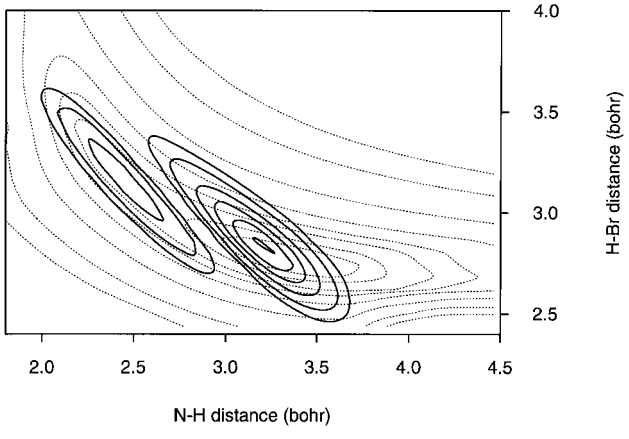

Figure 9. The square of the first excited dimer stretching vibrational wavefunction superimposed on the MP2/6-31+G(d, p) potential surface, with contours as in figure 7. The fundamental frequency is 218 cm^{-1}.

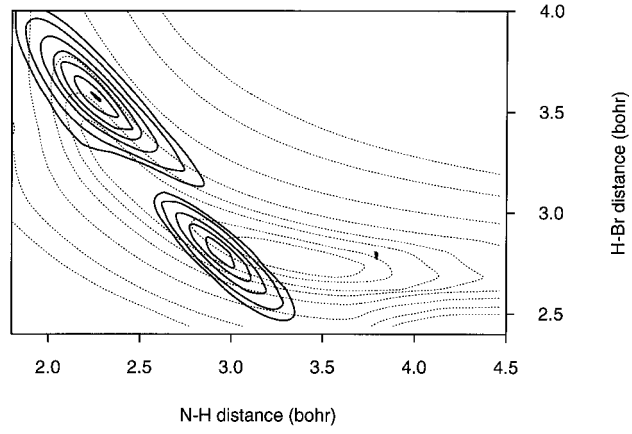

Figure 10. The square of the first excited proton stretching vibrational wavefunction superimposed on the MP2/6-31+G(d, p) potential surface, with contours as in figure 7. The fundamental frequency is 888 cm^{-1}.

Table 3. Single-point binding energies of BrH:NH$_3$ complexes at MP2/6-31+G(d, p) geometries.

	Binding energy/(kcal mol^{-1})	
	BrH:NH$_3$ (T)	BrH:NH$_3$ (PS)
MP2/6-31+G(d, p)	10·0	9·1
MP2/aug′-cc-pVDZ	8·6	7·1
MP2/aug′-cc-pVTZ	8·5	7·0

binding energy to a greater extent. Thus the difference between the stabilities of BrH:NH_3 (T) and BrH:NH_3 (PS) increases from 0·9 kcal mol^{-1} at MP2/6-31+(d, p), to 1·5 kcal mol^{-1} at MP2/aug′-cc-pVDZ. Further extension of the basis set leads to a lowering of the binding energies of both complexes by only 0·1 kcal mol^{-1}, keeping the energy difference between them the same. These results suggest that MP2/aug′-cc-pVDZ is an appropriate level of theory for re-examining the BrH:NH_3 potential surface. If the region on the potential surface corresponding to the proton-shared complex is raised in energy, then BrH:NH_3 will be more confined to the BrH:NH_3 (T) well. It will then be better described as a traditional hydrogen-bonded complex, and the expectation value of R_0 should increase.

The fully optimized BrH:NH_3 complex at MP2/aug′-cc-pVDZ is structurally and spectroscopically similar to BrH:NH_3 (T) at MP2/6-31+G(d, p). It has a slightly shorter intermolecular Br–N distance R_e of 3·216 Å and a Br–H distance of 1·481 Å. The binding energy of the fully optimized structure is 8·6 kcal mol^{-1}. The harmonic Br–H stretching frequency of 1980 cm^{-1} is similar to the MP2/6-31+G(d, p) value for BrH:NH_3 (T). No equilibrium structure corresponding to BrH:NH_3 (PS) was found on this surface, although there is a shoulder in the potential curve for proton transfer similar to, but higher in energy than, that found on the MP2/6-31+G(d, p) surface.

Following the procedure outlined above, another global BrH:NH_3 potential energy surface was obtained from 225 single-point calculations carried out at MP2/aug′-cc-pVDZ. The initial data points are illustrated in figure 11, and the resulting potential surface is shown in figure 12, with the global minimum indicated by an asterisk. The ground-state wavefunction calculated from this surface is illustrated in figure 13 and has an

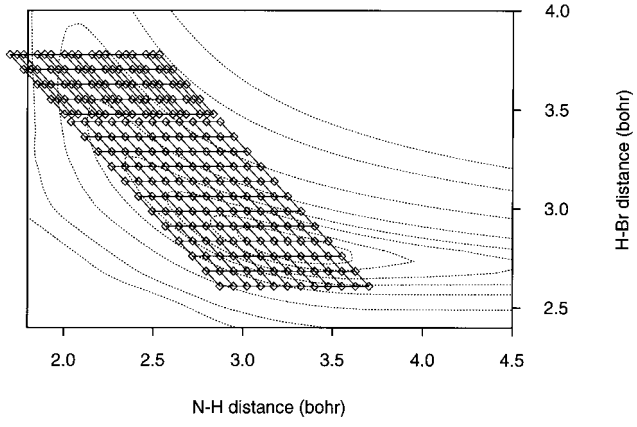

Figure 11. The MP2/aug′-cc-pVDZ potential energy surface for BrH:NH_3. The initial *ab initio* points used to define the surface are indicated.

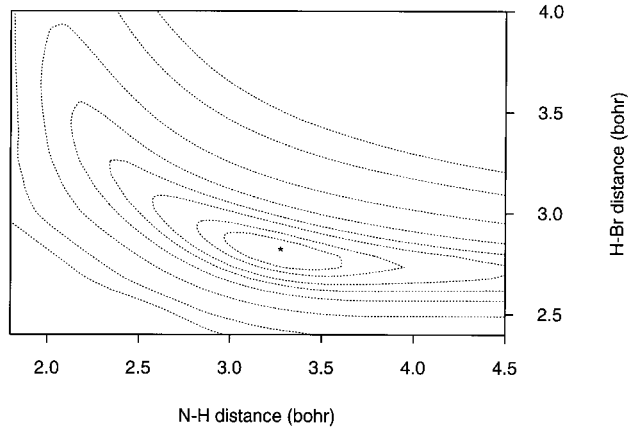

Figure 12. The potential energy surface for BrH:NH_3 at the MP2/aug′-cc-pVDZ level of theory with the global minimum indicated as an asterisk. Potential energy contours are as in figure 7.

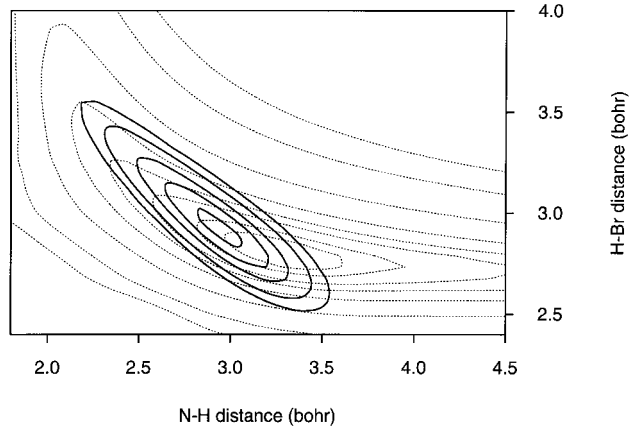

Figure 13. The square of the ground-state vibrational wavefunction superimposed on the MP2/aug′-cc-pVDZ potential surface, with contours as in figure 7. The zero-point energy is 920 cm^{-1}.

anharmonic zero-point energy of 2·6 kcal mol^{-1}. This wavefunction also exhibits large-amplitude motion over the hydrogen-bonding region of the potential energy surface although, as expected, the ground-state wavefunction lies closer to the BrH:NH_3 (T) well. The expectation value of the Br–N distance R_0 is 3·10 Å, slightly larger than that found on the MP2/6-31+G(d, p) surface. The relative increase in energy of the proton-shared configuration over the traditional BrH:NH_3 structure also increases the proton stretching vibrational eigenvalues. The anharmonic fundamental frequencies for the dimer stretching mode and the proton stretching mode are now 176 and 1106 cm^{-1} respectively. The corresponding wavefunctions are illustrated in figures 14 and 15. Table 2 summarizes the anharmonic results at MP2/aug′-cc-pVDZ.

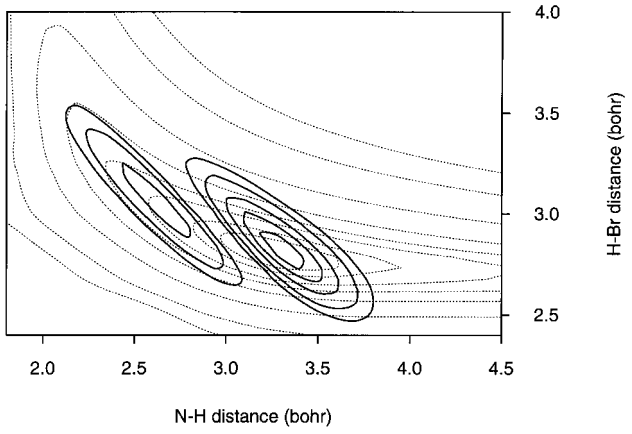

Figure 14. The square of the first excited dimer stretching vibrational wavefunction superimposed on the MP2/aug′-cc-pVDZ potential surface, with contours as in figure 7. The fundamental frequency is 176 cm^{-1}.

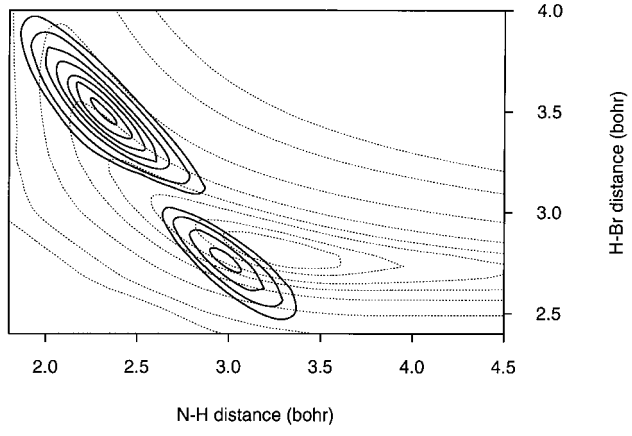

Figure 15. The square of the first excited proton stretching vibrational wavefunction superimposed on the MP2/aug′-cc-pVDZ potential surface, with contours as in figure 7. The fundamental frequency is 1106 cm^{-1}.

Although still larger than experiment, the anharmonic frequency is again much smaller than the harmonic approximation at 1980 cm^{-1}. Some of the differences between the theoretical and experimental results may arise from the model triatomic systems used or neglect of the Br–H–NH$_3$ bending motion. For this degree of freedom to be investigated, bending terms would need to be added to the potential energy surface and a three-dimensional Hamiltonian considered (for example [14]).

Another source of the discrepancy may be the argon matrix. Because of the presence of the argon atoms, it was not possible to obtain a global two-dimensional surface for BrH:NH$_3$:3Ar. Instead, one-dimensional anharmonic wavefunctions were calculated along the harmonic normal mode displacement vector for the

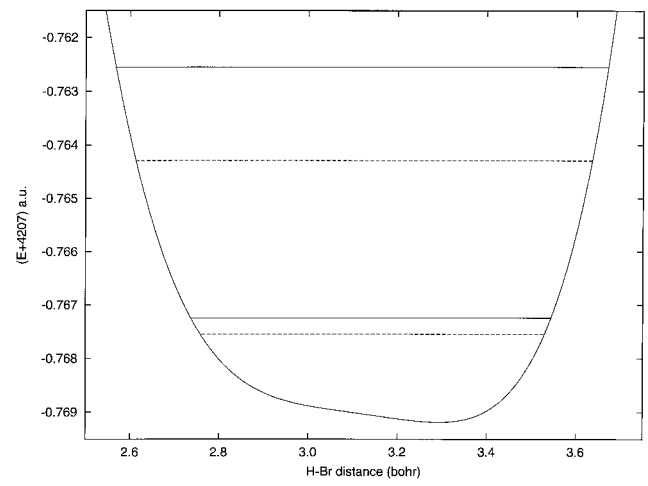

Figure 16. The potential energy and anharmonic vibrational energy levels (———) together with the harmonic levels (– – –) along the proton stretching normal mode displacement vector for BrH:NH$_3$:3Ar, parameterized by the H–Br distance.

proton stretching vibration. The calculated zero-point energy is 427 cm^{-1} (i.e. 1·22 kcal mol^{-1}) and the fundamental transition occurs at 1030 cm^{-1}. These energy levels, together with the harmonic approximations and the potential energy, are illustrated along the normal mode displacement vector in figure 16. The harmonic zero-point energy is relatively close to the anharmonic value, but the harmonic approximation significantly underestimates the true energy of the $v = 1$ state. The harmonic approximation is not as poor for BrH:NH$_3$:3Ar as for BrH:NH$_3$ owing to the flatness of the potential curve near the minimum in the complex with the argon atoms. Nevertheless, the agreement between the computed harmonic spectrum of BrH:NH$_3$:3Ar and the experimental BrH:NH$_3$ spectrum obtained in an argon matrix (see figure 3) must be viewed as fortuitous.

At this point it is instructive to compare similar one-dimensional eigenvalues with two-dimensional eigenvalues calculated from the MP2/6-31+G(d, p) surface. Along the proton stetching normal mode displacement vector, the zero-point energy is approximately 170 cm^{-1} higher than the two-dimensional value, and the fundamental transition is approximately 640 cm^{-1} higher in energy. Coupling of the dimer stretch with the proton stretch would thus be expected to reduce the anharmonic proton stretching eigenvalues on the BrH:NH$_3$:3Ar surface, bringing the anharmonic frequency into better agreement with experiment.

How do argon atoms influence the structure and vibrational spectrum of BrH:NH$_3$? Some insight into the role of these atoms can be obtained by examining figure 4. Plotted in this figure are MP2/6-31+G(d, p)

potential curves for proton motion along the normal coordinate for the Br–H stretch in $BrH:NH_3$(T) as a function of electric field strength. Going from top to bottom in this figure, the curves correspond to increasing field strength in the Br–H direction, beginning with no field and increasing the field in steps of 0·0025 au. The corresponding curves for $BrH:NH_3$ (T) generated at MP2/aug′-cc-pVDZ are similar. It is apparent from figure 4 that the introduction of a field has both qualitative and quantitative effects, converting the double minimum to a simple minimum, and stabilizing $BrH:NH_3$ (PS) relative to $BrH:NH_3$ (T). Even the weakest field of 0·0025 au alters the relative stabilities of the two $BrH:NH_3$ complexes and, as the field strength increases, the single minimum moves toward a proton-shared and then an ion-pair structure. The electric field preferentially stabilizes the more polar form of $BrH:NH_3$.

The field effects illustrated in figure 4 suggest a possible explanation for the effect of the argon atoms. The equilibrium complex $BrH:NH_3$ (T) is a polar complex with a large dipole moment μ_e = 4·79 D at MP2/6-31+G(d, p). The argon atoms surrounding this complex can be polarized by it and, in turn, these atoms can further polarize the complex. The polarization by the field tends to move the hydrogen-bonded proton toward the nitrogen atom to form $BrH:NH_3$ (PS), which has a computed dipole moment μ_e = 8·40 D. This movement is not costly energetically, since the potential surface is quite flat in the hydrogen-bonded region. The field calculations suggest that even a weak field, one which could be generated by polarized argon atoms, is sufficient to effect this change. For example, classical dipole/induced-dipole and charge/induced-dipole calculations predict that, in the presence of three argon atoms, the additional stabilization energy of the proton-shared structure is 1 and 3 kcal mol^{-1} respectively. These estimates are consistent with the *ab initio* result of 2 kcal mol^{-1}. It is anticipated that argon matrix effects will be important when the regions corresponding to the traditional and proton-shared complexes are energetically similar. In $BrH:NH_3$, the difference is about 1–1·5 kcal mol^{-1}.

Two decades ago, Zundel [24] discussed field and solvation effects on hydrogen-bonded complexes and made some interesting observations. He noted that potentials for hydrogen-bonded systems can be deformed by electric fields. He also noted that hydrogen bonds with double minima or a flat broad potential well are extremely polarizable, and that a large polarizability enhances interaction with the environment. Zundel's statements are appropriate to the $BrH:NH_3$ complex in an argon matrix.

4. Conclusions

The $BrH:NH_3$ complex has been investigated in an attempt to resolve the discrepancy between its computed vibrational spectrum and the experimental infrared spectrum in an argon matrix. The $BrH:NH_3$ equilibrium structure at MP2/6-31+G(d, p) and MP2/aug′-cc-pVDZ has a traditional hydrogen bond. Its vibrational spectrum, computed in the usual harmonic approximation, has a single strong band near 2000 cm^{-1}. The experimental spectrum obtained in an argon matrix at 10 K is more characteristic of a proton-shared hydrogen bond, with a strong absorption at 729 cm^{-1}. Observations of the infrared spectrum of gaseous $BrH:NH_3$ would be of interest.

The $BrH:NH_3$ potential surface is flat in the hydrogen-bonding region. As a result, the proton can undergo large-amplitude anharmonic motion even in the ground vibrational state. This motion samples both the traditional and the proton-shared hydrogen-bonding regions. Solving the two-dimensional nuclear vibrational problem for the dimer stretching and proton stretching modes shows that these motions are highly coupled. The computed anharmonic proton stretching frequencies are reduced by 1100 and 900 cm^{-1} at MP2/6-31+G(d, p) and MP2/aug′-cc-pVDZ respectively, relative to the corresponding harmonic frequencies. While these anharmonic frequencies are in better agreement with the experimental frequency in an argon matrix, they still overestimate the experimental value.

The MP2/6-31+G(d, p) structure of the $BrH:NH_3:3Ar$ complex has a proton-shared hydrogen bond, and a computed harmonic proton stretching frequency in agreement with experiment. However, the computed MP2/6-31+G(d, p) anharmonic frequency obtained by solving a one-dimensional nuclear Schrödinger equation is higher than the harmonic frequency, so the harmonic result is fortuitous. The argon matrix effect on the structure and spectrum of $BrH:NH_3$ is attributable to a field effect which preferentially stabilizes the more polar proton-shared structure. The significance of anharmonicity and matrix effects for $BrH:NH_3$ is akin to the fact that the traditional and proton-shared regions of the potential energy surface are energetically similar and easily accessible.

The harmonic approximation is a poor approximation for describing the large-amplitude proton motion in $BrH:NH_3$ and the coupling between the dimer and proton stretching modes. These modes require an anharmonic treatment. The remaining discrepancies between the two-dimensional model anharmonic calculations and the experimental data most probably arise from ignoring coupling to bending vibrations and from the difficulty in modelling the argon matrix effects.

Although the anharmonic vibrational calculations may be systematically improved, there is no obvious way to model accurately the argon matrix in these calculations.

Dedication

John Pople's first contributions to molecular physics were in the theory of liquids. His work with Lennard-Jones on hydrogen bonding in water proved highly influential and underpins much of our current understanding of the theory of hydrogen bonding. It is a pleasure to acknowledge this debt and to dedicate the present paper to him.

J.E.D.B. would like thank the National Science Foundation for grant No. CHE-9505888, the Ohio Supercomputer Center for computational support, and the Chemistry Department of the University of Cambridge for hospitality during her sabbatical visit. M.J.T.J. would like to acknowledge the financial support of a Research Fellowship from Girton College Cambridge and to thank Dr Esa Kauppi for invaluable assistance with the anharmonic vibrational eigenvalue calculations. The authors also acknowledge Dr Stuart Carter for helpful discussions and advice, Dr Willis Person and Dr Krystyna Szczepaniak for supplying the argon matrix spectrum of BrH:NH$_3$, and Dr Thom Dunning, Jr, for providing the bromine aug-cc-pVDZ basis set prior to its publication.

References

[1] Del Bene, J. E., and Shavitt, I., 1997, *Intermolecular Interactions: From van der Waals to Strongly-Bound Complexes*, edited by S. Scheiner (Chichester, West Sussex: Wiley), pp. 157–179.
[2] Howard, N. W., and Legon, A. C., 1987, *J. chem. Phys.*, **86,** 6722.
[3] Pople, J. A., Binkley, J. S., and Seeger, R., 1976, *Int. J. quantum. Chem. Symp.*, **10,** 1.
[4] Krishnan, R., and Pople, J. A., 1978, *Int. J. quant. Chem.*, **14,** 91.
[5] Bartlett, R. J., and Silver, D. M., 1975, *J. chem. Phys.*, **62,** 3258.
[6] Bartlett, R. J., and Purvis, G. D., 1978, *Int. J. quant. Chem.*, **14,** 561.
[7] Hehre, W. J., Ditchfield, R., and Pople, J. A., 1972, *J. chem. Phys.*, **56,** 2257.
[8] Hariharan, P. C., and Pople, J. A., 1973, *Theor. chim. Acta*, **28,** 213.
[9] Spitznagel, G. W., Clark, T., Chandrasekhar, J., and Schleyer, P. v. R., 1982, *J. comput. Chem.*, **3,** 363.
[10] Clark, T., Chandrasekhar, J., Spitznagel, G. W., and Schleyer, P. v. R., 1983, *J. comput. Chem.*, **4,** 294.
[11] Dunning, T. H., Jr, 1989, *J. chem. Phys.*, **90,** 1007.
[12] Kendall, R. A., Dunning, T. H., Jr, and Harrison, R. J., 1992, *J. chem. Phys.*, **96,** 6796.
[13] Woon, D. E., and Dunning, T. H., Jr, 1993, *J. chem. Phys.*, **98,** 1358.
[14] Wei, H., and Carrington, T., Jr, 1992, *J. chem. Phys.*, **97,** 3029.
[15] Diestler, D. J., and McKoy, V., 1968, *J. chem. Phys.*, **48,** 2951.
[16] Bouteiller, Y., Mijoule, C., Karpfen, A., Lischka, H., and Schuster, P., 1987, *J. phys. Chem.*, **91,** 4464.
[17] Mündel, C., and Domcke, W., 1984, *J. Phys.* B, **17,** 3593.
[18] Kauppi, E., 1994, *Chem. Phys. Lett.*, **229,** 661.
[19] *NAG Fortran Library—Mark 15*, 1991 (Oxford: Numerical Algorithms Group).
[20] Frisch, M. J., Trucks, G. W., Schlegel, H. B., Gill, P. M. W., Johnson, B. G., Robb, M. A., Cheeseman, J. R., Keith, T. A., Petersson, G. A., Montgomery, J. A., Raghavachari, K., Al-Laham, M. A., Zakrzewski, V. G., Ortiz, J. V., Foresman, J. B., Cioslowski, J., Stevfanov, B. B., Nanayakkara, A., Challacombe, M., Peng, C. Y., Ayala, P. Y., Chen, W., Wong, M. W., Andres, J. L., Replogle, E. S., Gomperts, R., Martin, R. L., Fox, D. J., Binkley, J. S., DeFrees, D. J., Baker, J., Stewart, J. P., Head-Gordon, M. Gonzalez, C., and Pople, J. A., 1995, *Gaussian 94* (Pittsburgh, PA: Gaussian, Inc.).
[21] Johnson, B. G., Gill, P. M. W., Head-Gordon, M., White, C. A., Baker, J., Maurice, D. R., Adamson, R. D., Adams, T. R., Oumi, M., and Ishikawa, N., 1997, *Q-Chem. 1.0* (Pittsburgh, PA: Q-Chem Inc.).
[22] Latajka, Z., Scheiner, S., and Ratajczak, H., 1992, *Chem. Phys.*, **166,** 85.
[23] Del Bene, J. E., Person, W. B., and Szczepaniak, K., 1996, *Molec. Phys.*, **89,** 47.
[24] Zundel, G., 1976, *The Hydrogen Bond,* Vol. II, edited by P. Schuster, G. Zundel and C. Sandorfy (Amsterdam: North-Holland), pp. 683–766.